Research Square

Preprints are preliminary reports that have not undergone peer review.
They should not be considered conclusive, used to inform clinical practice,
or referenced by the media as validated information.

Structural Effects on Thermal Stability and Photoluminescence of Novel Aromatic Poly(amide-imide)s Based on 3,4'-Bis(3-N-trimellitimido)chalcone and Various Aromatic Diamines

Matin Varcheh

matinvarche1365@gmail.com

Arak University https://orcid.org/0009-0009-0226-306X

Khalil Faghihi

Research Article

Keywords: Poly(amide-imide)s, Chalcone, Asymmetric diacid, Thermal stability, Photoluminescence, Structure–property relationship

Posted Date: November 10th, 2026

DOI: https://doi.org/10.21203/rs.3.rs-11418363/v1

License: This work is licensed under a Creative Commons Attribution 4.0 International License.
Read Full License

Structural Effects on Thermal Stability and Photoluminescence of Novel Aromatic Poly(amide-imide)s Based on 3,4′-Bis(3-N-trimellitimido)chalcone and Various Aromatic Diamines

Matin Varcheh[a] , Khalil Faghihi[a*]

[a]Organic Polymer Chemistry Research Laboratory, Department of Chemistry, Faculty of Science, Arak University, 38158-879, Arak, Iran.

Abstract

A novel series of aromatic poly(amide-imide)s (PAI-01–PAI-04) was synthesized from a novel asymmetric chalcone-based diimide-diacid and four structurally different aromatic diamines to investigate the effects of chain asymmetry and conjugation on thermal and optical properties. The key monomer, 3,4′-bis(3-N-trimellitimido)chalcone (6), was prepared in a two-step route: aldol condensation of 3-nitrobenzaldehyde and 4-nitroacetophenone to yield 4,3′-dinitrochalcone, followed by reduction with Fe/acetic acid to the corresponding diaminochalcone and subsequent imidization with trimellitic anhydride. The resulting PAIs were characterized by FT-IR and ^{1}H NMR, and their properties were evaluated by UV–Vis, photoluminescence (PL), XRD, TGA, and DTG. UV–Vis spectra exhibited primary absorption in the 250–264 nm range. Upon excitation at 365 nm, PAI-01, PAI-03, and PAI-04 emitted primarily at 404.5 nm, whereas PAI-02 showed a red-shifted emission at 425.8 nm. Thermal analysis revealed that PAI-02 possessed the highest char yield (59.8% at 800 °C) and a maximum degradation temperature (DTG_max) of 528.3 °C, while PAI-01 showed the highest T_{10}% (508 °C). XRD patterns indicated predominantly amorphous structures with localized short-range order. These findings demonstrate that the asymmetric chalcone-based diacid, combined with the diamine architecture, governs chain packing, thermal degradation pathways, and excited-state behavior. Among the synthesized polymers, PAI-02 is identified as the most promising candidate for applications requiring a combination of high thermal stability and blue-violet photoluminescence.

Keywords: Poly(amide-imide)s; Chalcone; Asymmetric diacid; Thermal stability; Photoluminescence; Structure–property relationship.

1- Introduction

High-performance aromatic polymers, especially poly(amide-imide)s (PAIs), have attracted considerable attention as advanced engineering materials because they combine the outstanding thermal and mechanical properties of polyimides with the processability and hydrogen-bonding capability of polyamides[1-3]. The simultaneous presence of rigid aromatic rings, polar carbonyl groups, and imide and amide units in the repeating unit imparts a unique combination of thermal resistance, chemical stability, mechanical strength, and, in some cases, electronic and optical functionality[1, 4]. Imide rings are known to play a decisive role in the thermal stability of the

backbone, whereas amide groups can enhance interchain cohesion through dipole–dipole interactions and hydrogen bonding[5]. Aromatic segments, on the other hand, increase chain rigidity and reduce segmental mobility[6, 7]. However, a higher degree of rigidity and aromaticity does not automatically guarantee improved thermal stability; the precise architecture of the repeating unit, the mode of linkage between rings, the presence of flexible or bulky side groups, molecular symmetry, and the capacity for intermolecular interactions all influence degradation behavior and char formation[8-10].

In recent years, the optical properties of aromatic polymers have also received increasing attention. Conjugated aromatic systems can act as chromophores; upon ultraviolet excitation, they generate excited states whose radiative decay can produce photoluminescence (PL)[1, 11-14]. The emission wavelength, intensity, and bandwidth are governed by factors such as electronic structure, degree of electron delocalization, charge-transfer character, local environment of the chromophore, and chain organization[15, 16]. Therefore, the design of polymer backbones that simultaneously provide high thermal stability and tunable optical behavior remains a challenging but attractive goal[17].

Among the various building blocks used for this purpose, chalcone (1,3-diaryl-2-propen-1-one) is particularly interesting because of its fully conjugated α,β-unsaturated ketone structure, photosensitivity, and good thermal stability[18-20]. Chalcone-containing polymers have been investigated as photosensitive materials, nonlinear optical materials, and fluorescent polymers[21, 22]. Incorporating chalcone units into a PAI backbone can extend conjugation and introduce additional electronic transitions, thereby influencing both thermal degradation pathways and photophysical behavior. Nevertheless, most reported chalcone-based poly(amide-imide)s have been prepared from symmetric monomers, and the effect of structural asymmetry on the resulting properties has not been systematically explored[23-25].

Introducing asymmetry into the diacid monomer is a promising strategy to modify chain packing, increase free volume, and alter interchain interactions without completely sacrificing thermal stability[26, 27]. An asymmetric diimide-diacid can restrict chain rotation, disrupt long-range ordering, and create heterogeneous chemical environments around the chromophores. When such a diacid is combined with different aromatic diamines, the resulting PAIs can exhibit distinct thermal stabilities, char yields, UV absorption, and PL emission. Despite these potential

advantages, a detailed structure–property study on asymmetric chalcone-derived diimide-diacids and their corresponding PAIs is still lacking[28-31].

In this work, a novel asymmetric diimide-diacid, 3,4′-bis(3-N-trimellitimido)chalcone (6), was synthesized from 3-nitrobenzaldehyde and 4-nitroacetophenone via a two-step route involving aldol condensation and subsequent reduction, followed by imidization with trimellitic anhydride. The resulting diacid was then reacted with four structurally different aromatic diamines to afford a series of poly(amide-imide)s designated PAI-01–PAI-04. The polymers were characterized by FT-IR and ^{1}H NMR, and their properties were evaluated using UV–Vis, PL, XRD, TGA, and DTG. The primary objective is not merely to report the individual performance of each polymer, but to establish a comparative structure–property relationship that elucidates how variations in diamine architecture, combined with the asymmetric chalcone-based diacid, influence thermal stability, char formation, UV absorption, photoluminescence, and crystallinity. Among the synthesized polymers, PAI-02 was identified as the most promising candidate for applications requiring a combination of high thermal stability and blue-violet photoluminescence.

2. Experimental

2.1. Materials

3-Nitrobenzaldehyde ($C_7H_5NO_3$), 4-nitroacetophenone ($C_8H_7NO_3$), trimellitic anhydride ($C_9H_4O_5$), ethanol (C_2H_5OH), pyridine (C_5H_5N), N,N-dimethylacetamide (DMAc), calcium chloride ($CaCl_2$), triphenyl phosphite ($P(OC_6H_5)_3$), N-methyl-2-pyrrolidone (NMP), and N,N-dimethylformamide (DMF) were purchased from Sigma-Aldrich Chemical Co. (USA) and Merck Chemical Co. (Germany). All reagents and solvents were used as received without further purification unless otherwise stated.

2.2. Characterization and Instrumentation

^{1}H NMR spectra were recorded on a Bruker Avance 300 MHz spectrometer (Germany) using DMSO-d_6 as solvent. Fourier transform infrared (FT-IR) spectra were obtained on a Galaxy series FTIR 5000 spectrophotometer (England) using KBr pellets. Vibrational frequencies are reported in the range 400–4000 cm^{-1}, and band intensities are designated as weak (w), medium (m), shoulder (sh), strong (s), and broad (br). Thermogravimetric analysis (TGA) and derivative thermogravimetry (DTG) were performed on a Mettler TA4000 system under a nitrogen

atmosphere at a heating rate of 10 °C min^{-1}. The progress of reactions was monitored by thin-layer chromatography (TLC) using a 60 W UV lamp. X-ray diffraction (XRD) patterns were recorded on a Philips X'pert diffractometer with Cu Kα radiation (λ = 0.15405 nm). A Memert 400 vacuum oven was used for drying samples. UV–Vis electronic spectra were recorded on a Specord S600 single-beam spectrometer and a PerkinElmer Lambda 15 double-beam spectrometer. Photoluminescence (PL) spectra were obtained using a [spectrofluorometer model] with an excitation wavelength of 365 nm. Inherent viscosities (η_inh) were measured with an Ostwald viscometer at 25 °C using DMSO as solvent at a concentration of 0.05 g dL^{-1}.

2.3. Monomer Synthesis

2.3.1. Synthesis of 4,3′-Dinitrochalcone (3)

A mixture of 3-nitrobenzaldehyde (1) (1.83 g, 12.1 mmol), 4-nitroacetophenone (2) (2.00 g, 12.1 mmol), and acetic anhydride (25 mL) was stirred and refluxed overnight. The reaction mixture was then poured into distilled water, and the resulting yellow-brown precipitate was filtered, washed thoroughly with water, and dried to afford 2.70 g of compound 3 (yield 75%). A purified sample was obtained by recrystallization from DMF. mp: 215.5–217 °C. FT-IR (KBr, cm^{-1}): 3107 (sp^2 C–H stretch), 1695 (C=O stretch, conjugated), 1532 (asym. NO_2 stretch), 1356 (sym. NO_2 stretch), 986 (=C–H out-of-plane bend).

2.3.2. Synthesis of 4,3′-Diaminochalcone (4)

4,3′-Dinitrochalcone (3) (2.00 g, 6.71 mmol) was dissolved in ethanol (40 mL), and iron powder (2.00 g) and acetic acid (20 mL) were added. The mixture was refluxed for 2 h. After cooling, the solution was made basic with 3 M NaOH until pH 8. The mixture was transferred to a 150 mL separatory funnel, and ethyl acetate (25 mL) was added. After shaking, the funnel was allowed to stand for 4 h to allow phase separation. The yellow organic phase was separated, washed with distilled water (3 × 15 mL), and then washed with brine (15 mL, 3 M). Anhydrous $MgSO_4 \cdot 7H_2O$ (2 g) was added to remove residual water. The clear solution was separated, and the solvent was removed using a water bath to yield 1.17 g of compound 4 (yield 74%). mp: 178–180 °C. FT-IR (KBr, cm^{-1}): 3200–3500 (N–H stretch), 1632 (C=O stretch, conjugated), 1000–1250 (C–N stretch, aromatic amine). The absence of bands at 1532 and 1356 cm^{-1} confirmed complete reduction of nitro groups.

2.3.3. Synthesis of 4,3′-Bis(3-N-trimellitimido)chalcone (6) – Diacid Monomer

A mixture of compound 4 (1.00 g, 4.2 mmol), trimellitic anhydride (5) (1.61 g, 8.4 mmol), and acetic acid (20 mL) was stirred at room temperature overnight and then refluxed for 4 h. Distilled water was added to complete precipitation. The precipitate was filtered, washed thoroughly with distilled water, and dried at room temperature to give 1.2 g of diacid 6 (yield 52%). Molecular weight: 550 g mol^{-1}. mp: 207.5–208.8 °C.

FT-IR (KBr, cm^{-1}): 1724 (C=O stretch, imide and acid), 1630–1660 (C=O stretch, ketone, overlapped), 3300–3500 (O–H stretch, acid).

2.4. Polymer Synthesis (PAI-01 to PAI-04)

The poly(amide-imide)s were synthesized by the solution polycondensation method. In a typical procedure, a mixture of diacid 6 (1 mmol) and the corresponding aromatic diamine (1 mmol) was placed in a flask equipped with a magnetic stirrer and a reflux condenser. Triphenyl phosphite (3 mL), pyridine (1 mL), NMP (9 mL), and calcium chloride (0.6 g) were added. The reaction mixture was heated gradually: 60 °C for 1 h, 90 °C for 3 h, and 110 °C for 5 h. After cooling to room temperature, the viscous solution was poured into an excess of methanol to precipitate the polymer. The precipitate was collected by filtration, washed with acetone, and dried under vacuum at 80 °C for 6 h. The same procedure was applied using the four different diamines (4a–d) to obtain PAI-01, PAI-02, PAI-03, and PAI-04.

2.5. Solubility and Viscosity Measurements

Solubility of the PAIs was tested at a concentration of 5 mg mL^{-1} in various polar and non-polar solvents (H_2O, C_2H_5OH, n-hexane, toluene, DMF, DMSO, DMAc, NMP) at room temperature and at 60 °C. Inherent viscosities were measured in DMSO at 25 °C using an Ostwald viscometer at a concentration of 0.05 g dL^{-1}.

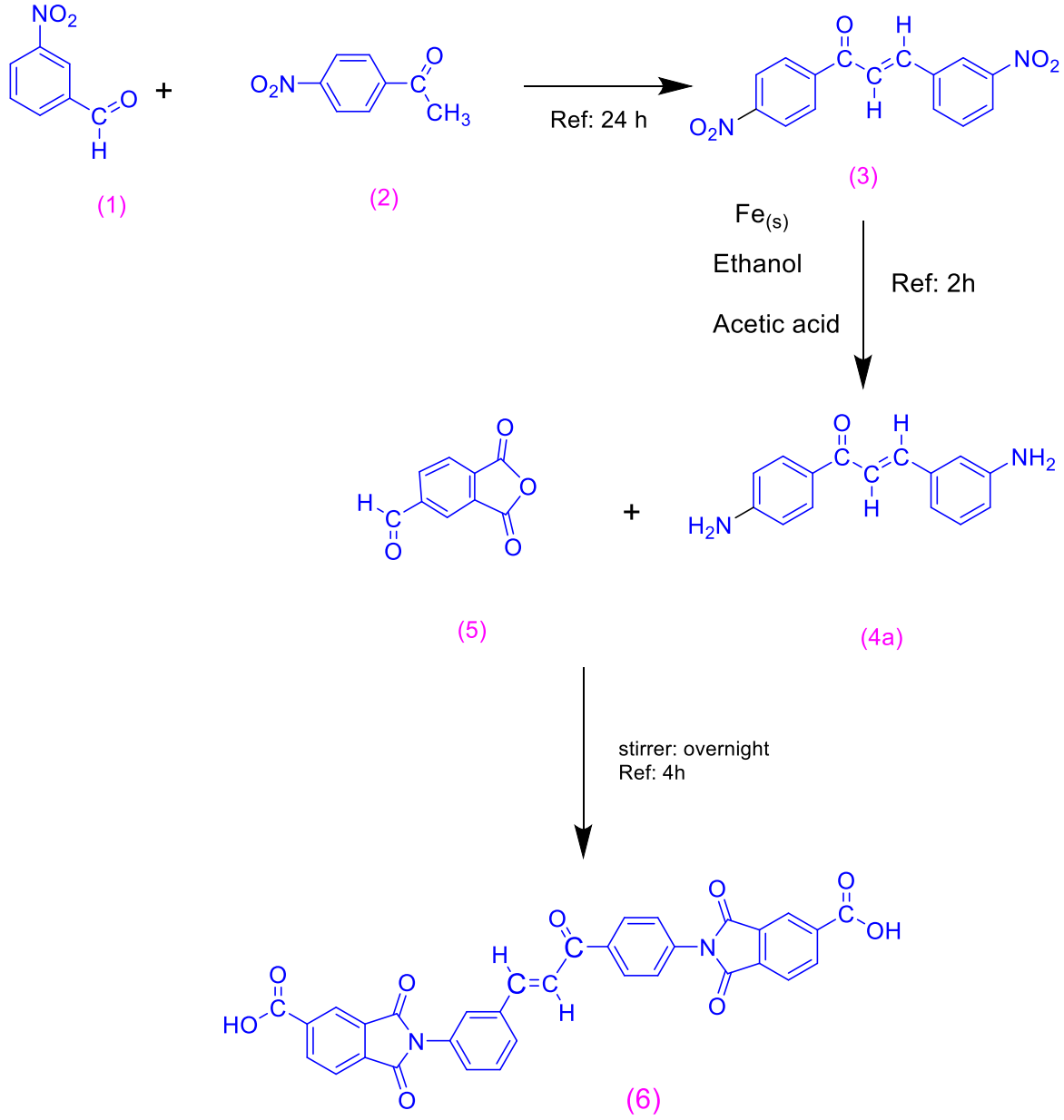
3.Result and discussion

Note: Figures 1, 2, and 3 (FT-IR spectra of compounds 3, 4, and 6) have been moved to the Supporting Information as Figures S1, S2, and S3, respectively. All references to these spectra in the main text now point to the Supporting Information.

3.1. Monomer Synthesis and Characterization

The synthetic route to the asymmetric diimide-diacid monomer (6) is outlined in Scheme 1. The key intermediate, 4,3′-dinitrochalcone (3), was prepared via aldol condensation between 3-nitrobenzaldehyde (1) and 4-nitroacetophenone (2) in acetic anhydride. The structure of compound 3 was confirmed by FT-IR spectroscopy (Supporting Information, Figure S1). The absorption band at 3107 cm^{-1} corresponds to sp^2 C–H stretching vibrations of the aromatic rings.

The carbonyl stretching vibration appears at 1695 cm^{-1}, shifted to a lower wavenumber compared to a typical ketone due to extensive conjugation with the adjacent C=C bond and the electron-withdrawing effect of the nitro groups. The strong asymmetric and symmetric NO_2 stretching vibrations are observed at 1532 and 1356 cm^{-1}, respectively. The out-of-plane bending vibration of the =C–H bond at 986 cm^{-1} confirms the trans configuration of the alkene, which is typical for chalcones.



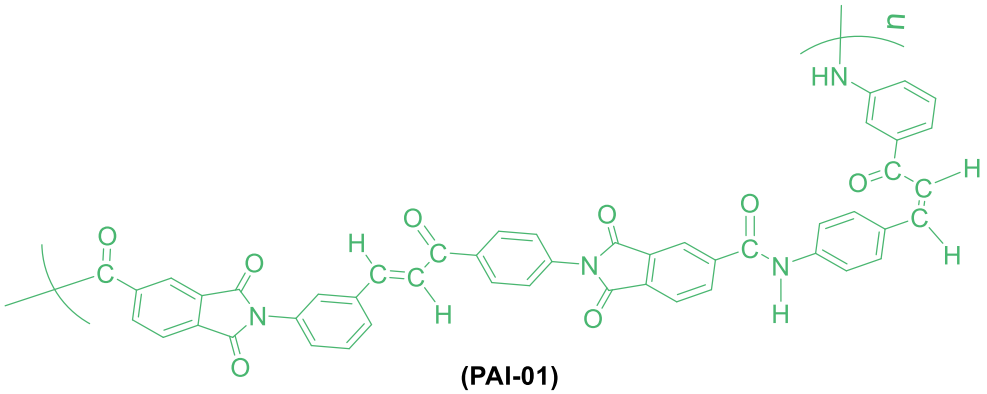
Scheme 1. Synthetic route to 3,4′-bis(3-N-trimellitimido)chalcone (6): (i) aldol condensation of 3-nitrobenzaldehyde (1) and 4-nitroacetophenone (2) in acetic anhydride; (ii) reduction of 4,3′-dinitrochalcone (3) with Fe/AcOH in ethanol; (iii) imidization of 4,3′-diaminochalcone (4) with trimellitic anhydride (5) in acetic acid.

Reduction of compound 3 with iron powder in an acidic medium afforded the corresponding diaminochalcone (4). The complete reduction of nitro groups was verified by FT-IR (Supporting Information, Figure S2). The disappearance of the asymmetric and symmetric NO_2 stretching bands at 1532 and 1356 cm^{-1}, together with the appearance of N–H stretching vibrations in the 3200–3500 cm^{-1} region and aromatic amine C–N stretching bands at 1000–1250 cm^{-1}, clearly confirms the formation of the amino groups. The carbonyl stretching vibration of the conjugated ketone appears at 1632 cm^{-1}.

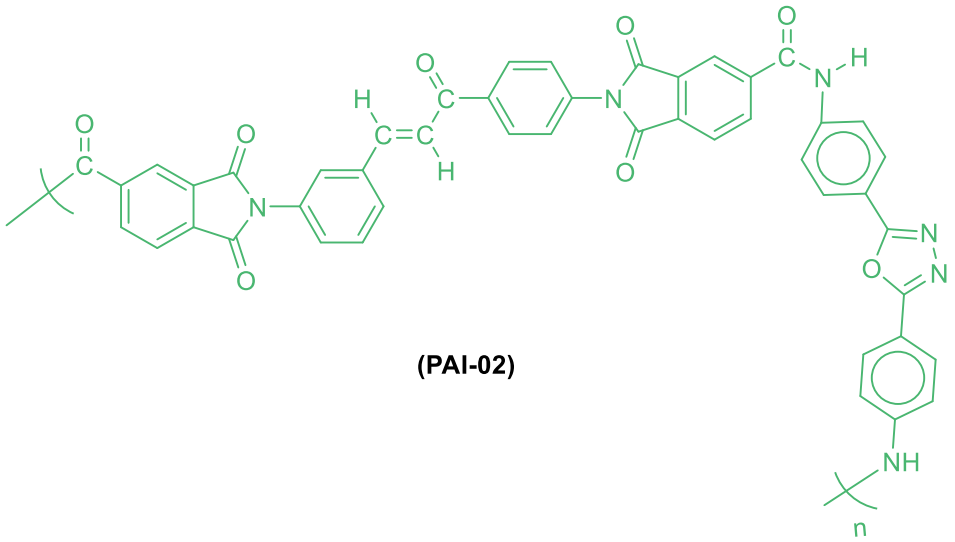
The diacid monomer (6) was synthesized by reacting compound 4 with trimellitic anhydride (5) in acetic acid. The FT-IR spectrum of compound 6 (Supporting Information, Figure S3) shows the disappearance of the N–H stretching bands and the appearance of characteristic imide and acid carbonyl absorptions. A sharp band at 1724 cm^{-1} is attributed to the overlapping C=O stretching vibrations of the imide and carboxylic acid groups. The ketone carbonyl band is observed in the 1630–1660 cm^{-1} region, partially overlapped with the aromatic ring vibrations. The broad band in the 3300–3500 cm^{-1} range corresponds to the O–H stretching of the carboxylic acid groups.

3.2. Polymer Synthesis and Structural Characterization

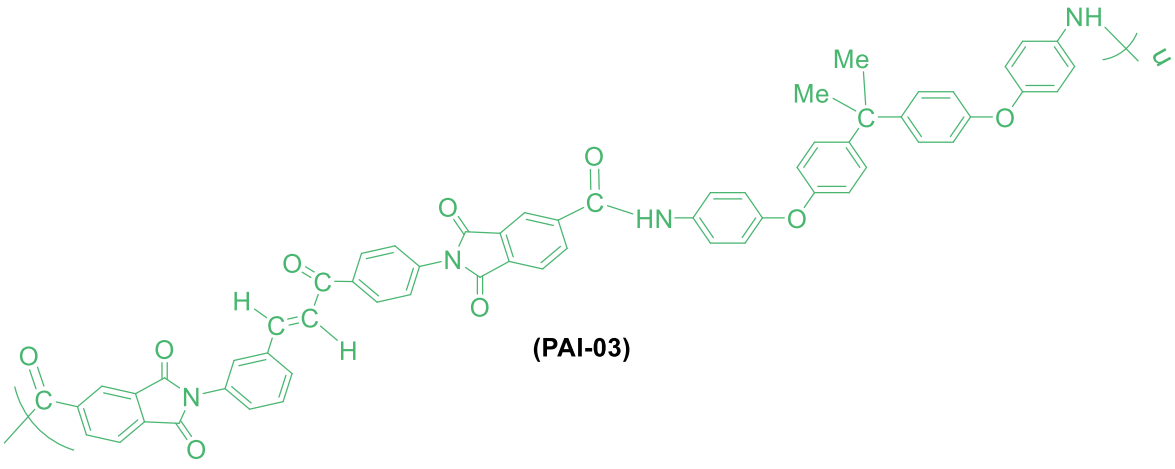
The poly(amide-imide)s PAI-01 to PAI-04 were synthesized by solution polycondensation of the diacid 6 with four structurally different aromatic diamines (4a–d) in the presence of triphenyl phosphite, pyridine, and calcium chloride in NMP. The structures of the repeating units are shown in Scheme 2. The diamines used are listed in Table 1.



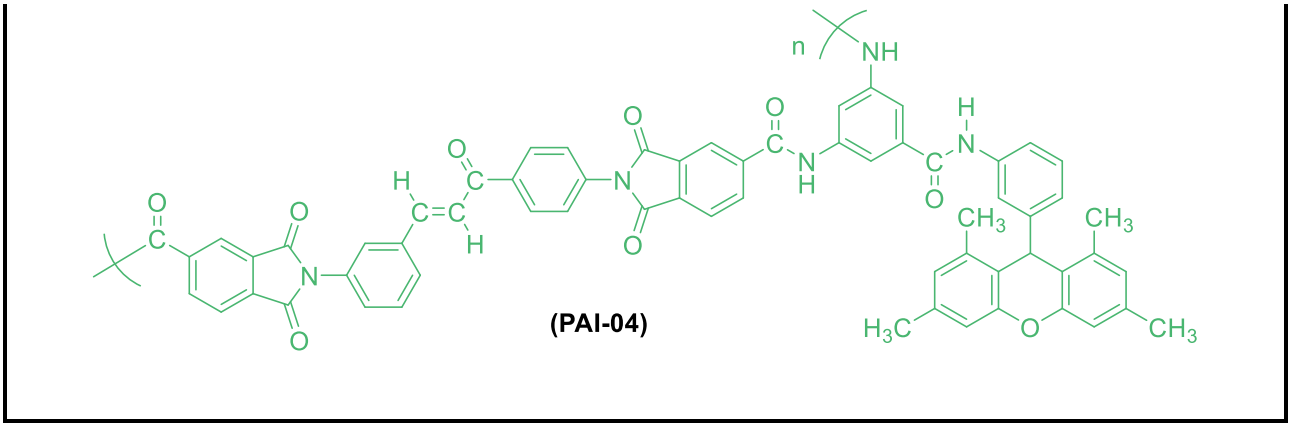
(PAI-01)



(PAI-02)

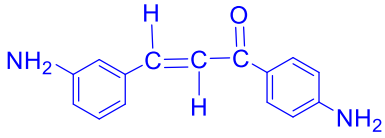
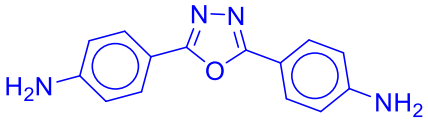
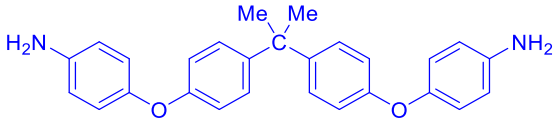
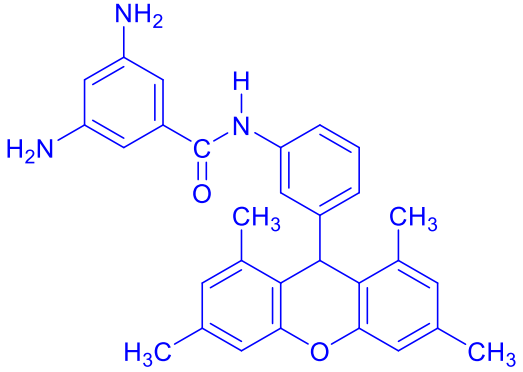


(PAI-03)



Scheme 2. Structures of the repeating units of the synthesized poly(amide-imide)s PAI-01 to PAI-04, obtained from the asymmetric diacid 6 and different aromatic diamines (4a–d).

Table 1. Structure of the aromatic diamines used for the synthesis of PAI-01 to PAI-04.

Diamin	Structure of diamine	Mv $_{(diamine)}$ g/mol	Diacid	product
4a		238	6	PAI-01
4b		252	6	PAI-02
4c		258	6	PAI-03
4d		463	6	PAI-04

The formation of the PAIs was confirmed by FT-IR spectroscopy (Figure 1). All four polymers exhibit characteristic imide absorptions at 1778 cm^{-1} (asymmetric C=O stretching) and 1724

cm^{-1} (symmetric C=O stretching), indicating successful imidization. The C–N stretching vibration of the five-membered imide ring appears at 1375 cm^{-1}, and the out-of-plane deformation of the imide ring is observed at 728 cm^{-1}. The amide N–H stretching vibration appears as a broad band centered at 3360 cm^{-1} (3300–3400 cm^{-1} region). The amide carbonyl stretching vibration is observed at 1660 cm^{-1}, while the combined N–H bending and C–N stretching vibrations of the amide group appear at 1540 cm^{-1}. Aromatic C=C skeletal vibrations are observed at 1490 and 1603 cm^{-1}, and aliphatic and aromatic C–H stretching vibrations appear in the 2850–2960 cm^{-1} region.

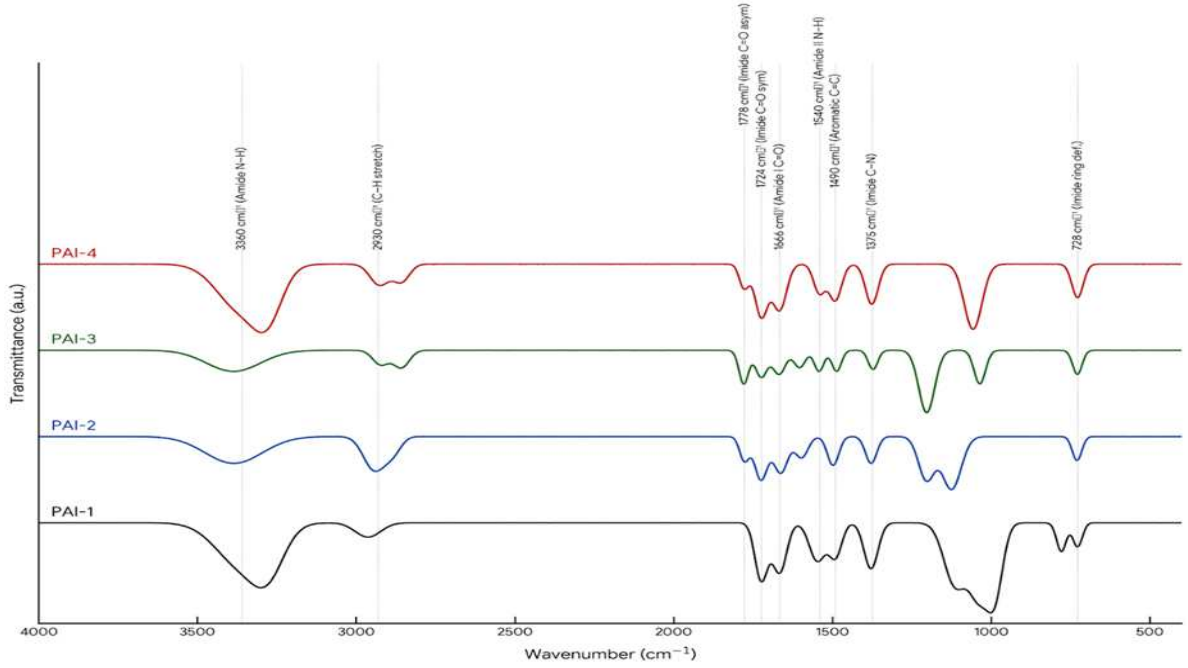


Figure 1. FT-IR spectra of the synthesized poly(amide-imide)s PAI-01, PAI-02, PAI-03, and PAI-04.

The FT-IR spectra confirm that the poly(amide-imide) backbone is preserved in all four polymers, while variations in the spectra reflect differences in the chemical environment of the functional groups, aromatic architecture, hydrogen bonding, and chain rigidity.

The ^{1}H NMR spectra of the PAIs (Figure 2) provide further structural evidence. Amide N–H protons appear in the 9–10.5 ppm range, appearing at lower fields due to the electron-withdrawing carbonyl group and hydrogen bonding. Aromatic protons resonate in the 6.5–8 ppm region as multiple signals, reflecting their presence in different chemical environments. Vinylic protons of the chalcone moiety appear in the 6.5–7.5 ppm range, partially overlapping with the

aromatic signals. For PAI-03, the two methyl groups in the diamine structure are in equivalent chemical environments and appear as a singlet in the 3.7–3.9 ppm range, shifted downfield due to the proximity of oxygen atoms.

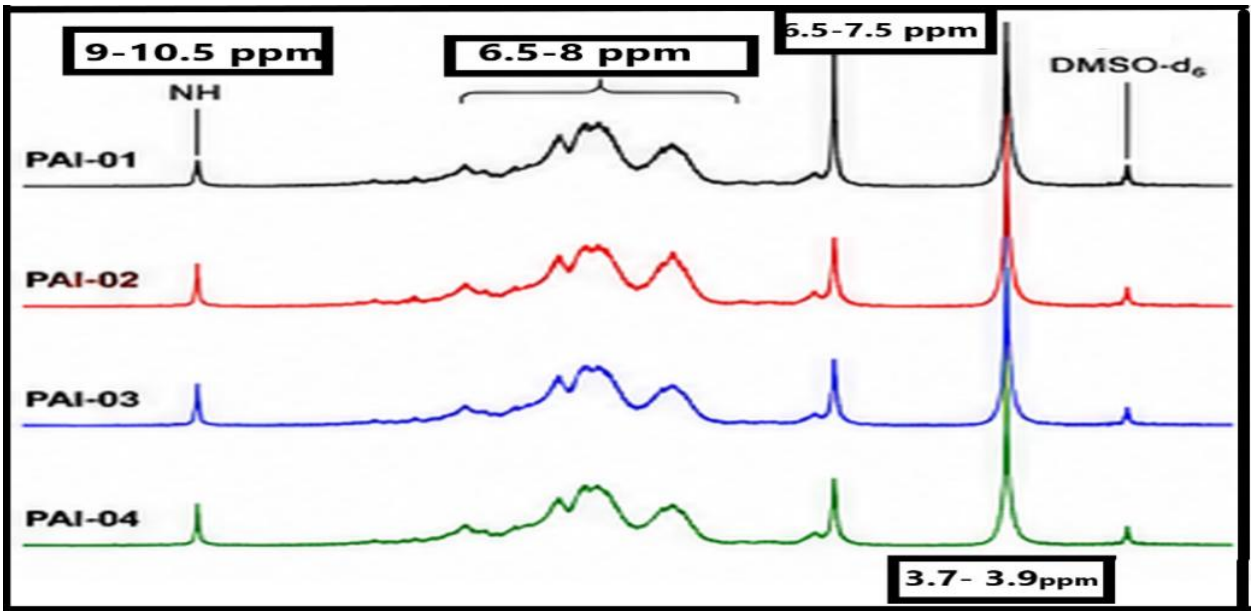


Figure 2. ^{1}H NMR spectra of PAI-01 to PAI-04 in DMSO-d_6. Amide N–H protons appear at 9–10.5 ppm, aromatic and vinylic protons at 6.5–8 ppm, and the methyl protons of PAI-03 as a singlet at 3.7–3.9 ppm.

The solubility behavior of the PAIs was investigated in various polar and non-polar solvents at a concentration of 5 mg mL^{-1} at both room temperature and 60 °C (Table 2). All polymers exhibited excellent solubility in polar aprotic solvents such as DMF, DMSO, DMAc, and NMP, which is attributed to strong dipole–dipole interactions between the polymer chains and the solvent. They were insoluble in water, ethanol, n-hexane, and toluene.

Table 2. Solubility behavior of PAI-01 to PAI-04.

PAI		H_2O	C_2H_5OH	n-Hexane	Toluene	DMF	DMSO	DMAc	NMP
01	Rt	-	-	-	-	+	+	+	+
	T_2	-	-	-	-	+	+	+	+
02	Rt	-	-	-	-	+	+	+	+
	T_2	-	-	-	-	+	+	+	+
03	Rt	-	-	-	-	+	+	+	+
	T_2	-	-	-	-	++	++	++	++
04	Rt	-	-	-	-	+	+	+	+
	T_2	-	- +	-	-	++	++	++	++

Solubility: – insoluble; + soluble; ++ excellent solubility. Tested at 5 mg mL^{-1} at room temperature and 60 °C. Please insert Table 2 with the complete data, as some entries in the original table are unclear.

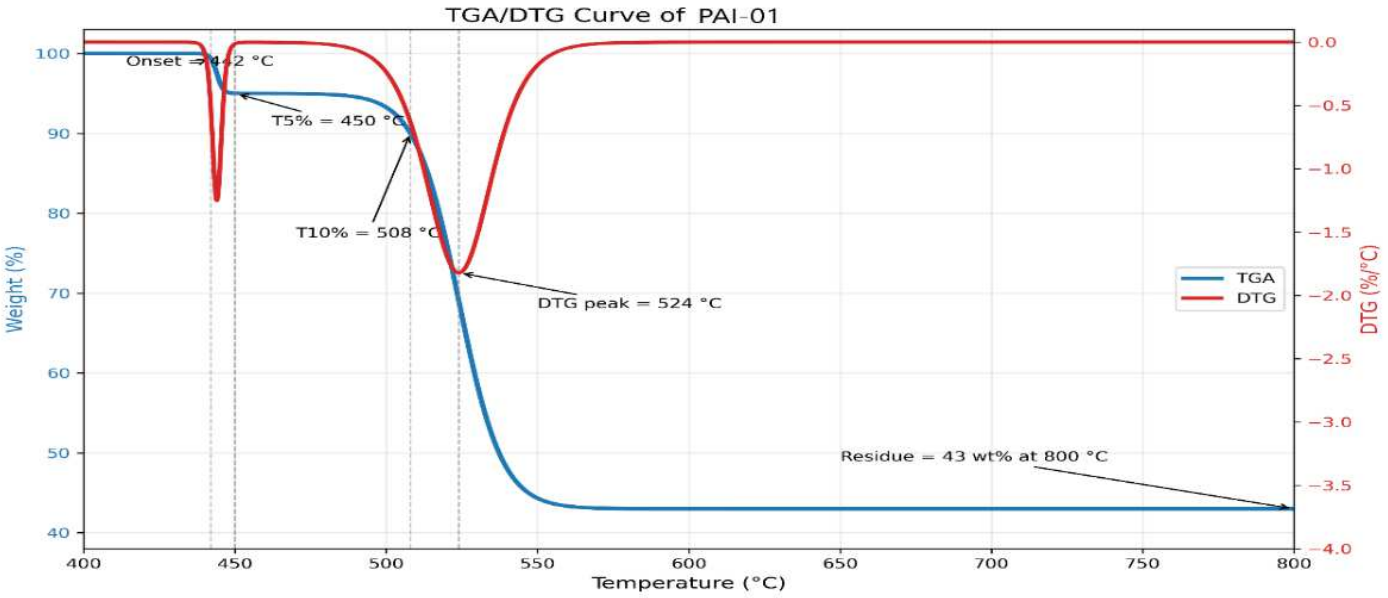
The inherent viscosities (η_inh) of the polymers were measured in DMSO at 25 °C at a concentration of 0.05 g dL^{-1} (Table 3). The value obtained for PAI-01 was 0.78 dL g^{-1}, indicating a suitable molecular weight and favorable processability.

Table 3. Inherent viscosity of PAI-01 to PAI-04.

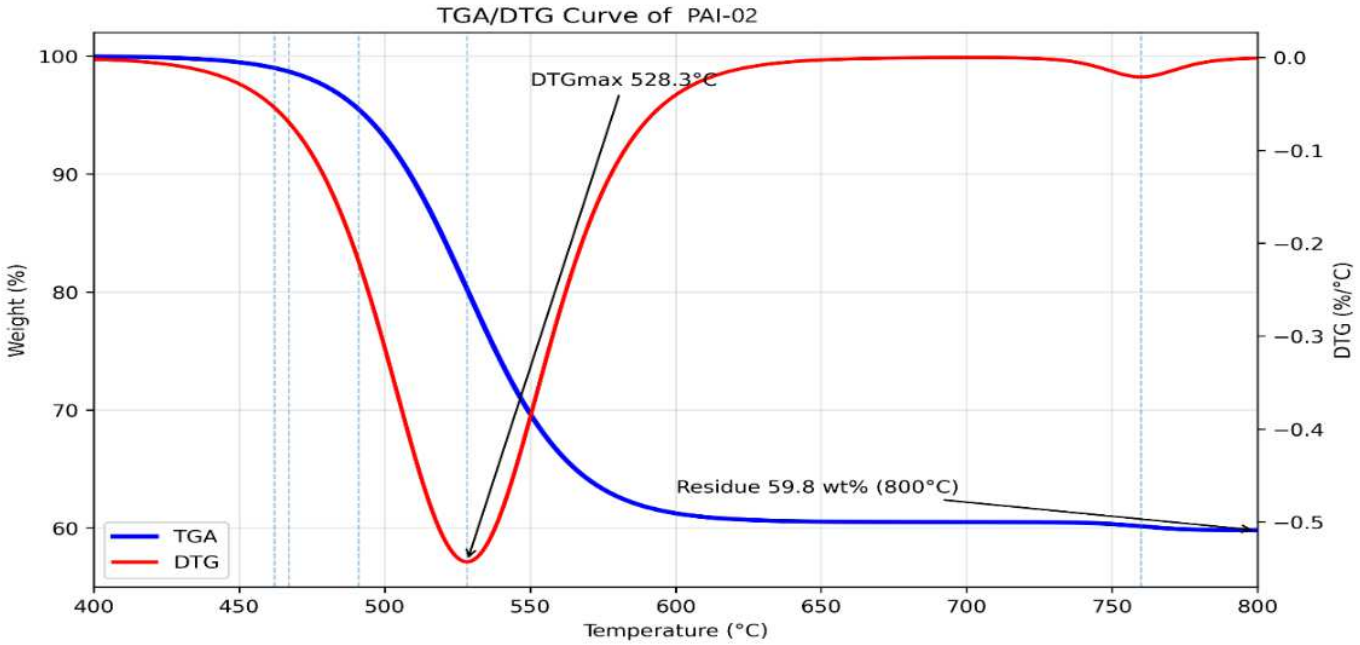
Polymer	η_inh (dL g^{-1})
PAI-01	0.78
PAI-02	0.43
PAI-03	0.54
PAI-04	0.83

3.3. Thermal Properties

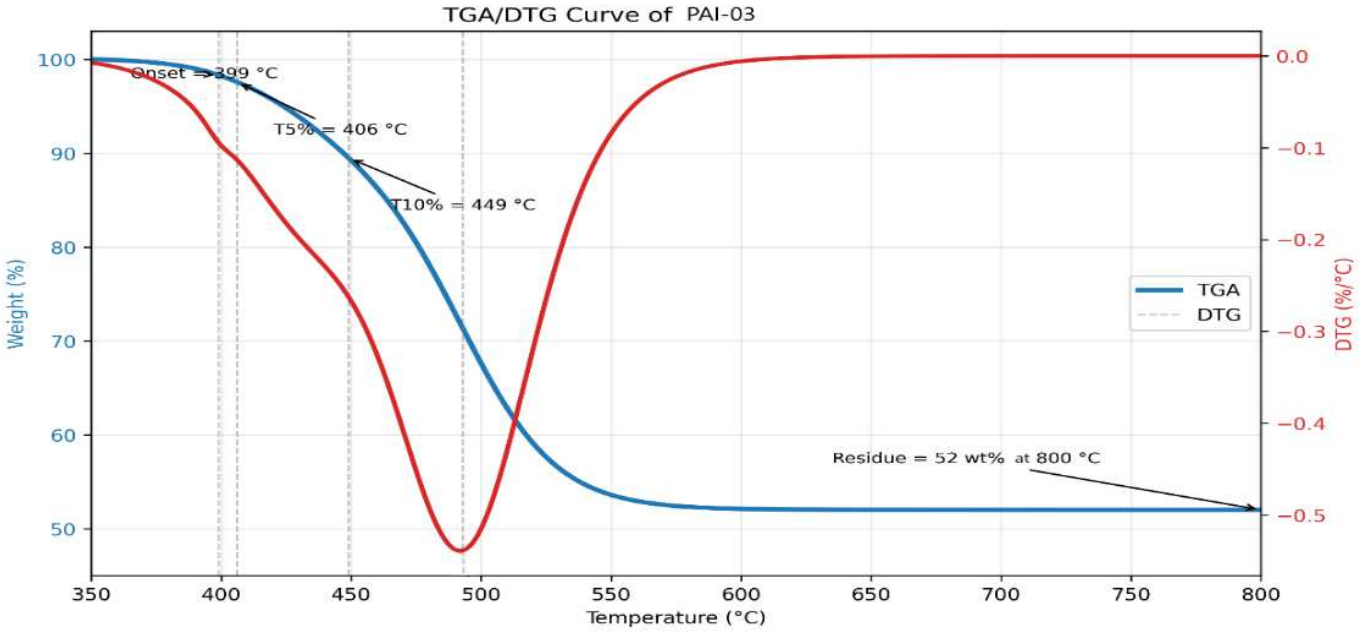
The thermal stability and degradation behavior of the PAIs were investigated by TGA and DTG under a nitrogen atmosphere. The results are summarized in Table 4, and the TGA/DTG curves are shown in Figures 3a–3d.



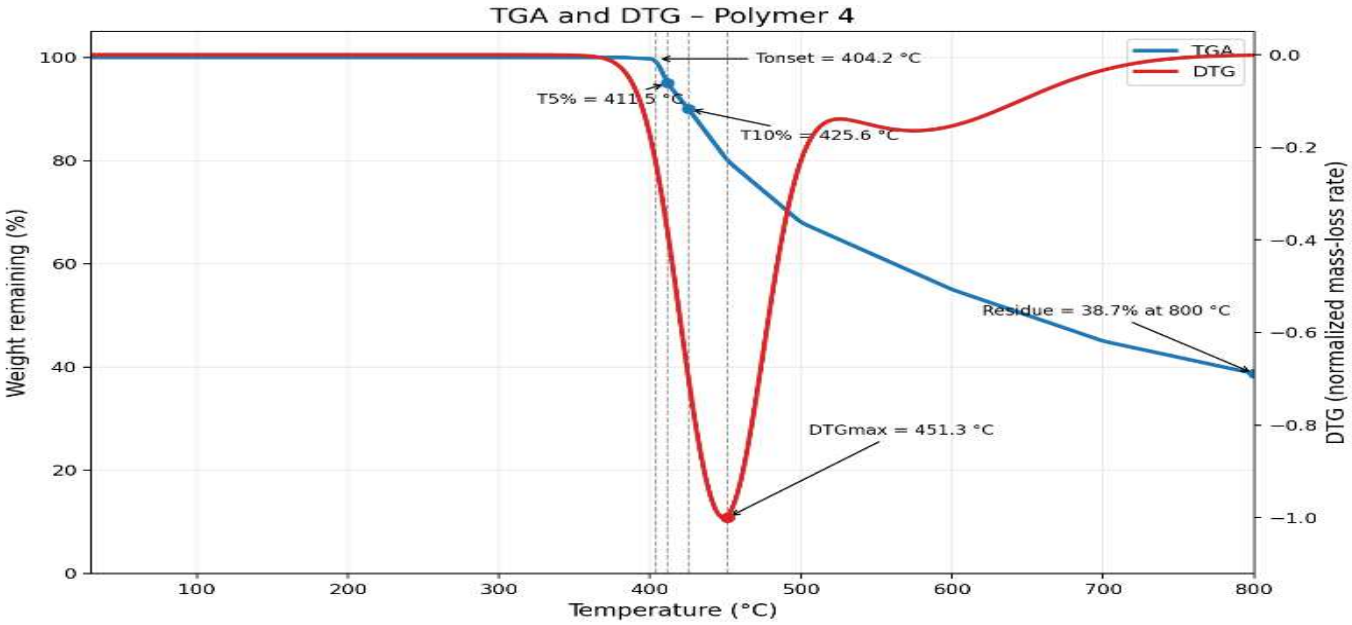
(a)


TGA/DTG Curve of PAI-02
DTGmax 528.3°C
Residue 59.8 wt% (800°C)
TGA
DTG
Weight (%)
DTG (%/°C)
Temperature (°C)

(b)


TGA/DTG Curve of PAI-03
Onset = 399 °C
T5% = 406 °C
T10% = 449 °C
Residue = 52 wt% at 800 °C
TGA
DTG
Weight (%)
DTG (%/°C)
Temperature (°C)

(c)



(d)

Figure 3. TGA and DTG curves of the synthesized poly(amide-imide)s: (a) PAI-01, (b) PAI-02, (c) PAI-03, and (d) PAI-04. Measurements were performed under N_2 at a heating rate of 10 °C min^{-1}.

Table 4. TGA and DTG data for PAI-01 to PAI-04.

PAIs	T onset (°C)	$T_{5\%}$ (°C)	$T_{10\%}$ (°C)	DTG_{max} (C)	Residue At 800 °C
PAI-01	442	450	508	524	43%
PAI-02	462	467	491	528.3	59.8%
PAI-03	399	406	449	493	52%
PAI-04	404.2	411.5	425.6	451.3	38.7%

All four polymers exhibited excellent thermal stability, with onset degradation temperatures above 400 °C. PAI-02 showed the highest thermal resistance, with the highest T_onset (462 °C), the highest DTG_max (528.3 °C), and the highest char yield at 800 °C (59.8%). This superior performance can be attributed to the greater rigidity of its polymer backbone, stronger interchain interactions, and a degradation pathway that favors carbon residue formation. In contrast, PAI-01 exhibited the highest T_{10}% value (508 °C), indicating that after the initial stage of degradation, it

resists further mass loss more effectively than PAI-02. This suggests that PAI-01 should not be considered inferior in thermal stability; rather, it possesses outstanding stability during the later stages of thermal degradation. The difference between T_onset and DTG_max for PAI-01 is 82 °C, for PAI-02 is 66.3 °C, for PAI-03 is 94 °C, and for PAI-04 is 47.1 °C. These values indicate that degradation is not an abrupt process but occurs over a temperature range, involving the sequential breakdown of different structural units.

PAI-03 exhibited the second-highest char yield (52%) despite having a lower T_onset (399 °C). This indicates that an earlier onset of degradation does not necessarily result in lower residue formation. PAI-04 showed the lowest thermal resistance among the four polymers, with a T_onset of 404.2 °C, a DTG_max of 451.3 °C, and a char yield of 38.7%. However, its onset degradation temperature above 400 °C still signifies considerable thermal resistance. The lower char yield of PAI-04 compared to PAI-02 demonstrates that alterations in chain architecture can have a greater impact on char formation than the mere presence of aromatic rings. The bulky aromatic moieties with methyl groups, oxygen atoms, and flexible segments in PAI-03 and PAI-04 create decomposition pathways that produce more volatile substances, reducing the final residue.

The asymmetric nature of the diacid monomer restricts chain rotation and mobility, enhancing the likelihood of forming stable aromatic carbon structures during degradation. The diacid structure and its asymmetric chain formation influence both the initiation of thermal breakdown and the ability to form stable residues at elevated temperatures.

The overall structure–property relationships established in this work are summarized in Figure 4, which illustrates how the asymmetric chalcone-based diacid, combined with different diamine architectures, governs thermal stability, char formation, UV absorption, photoluminescence, and crystallinity.

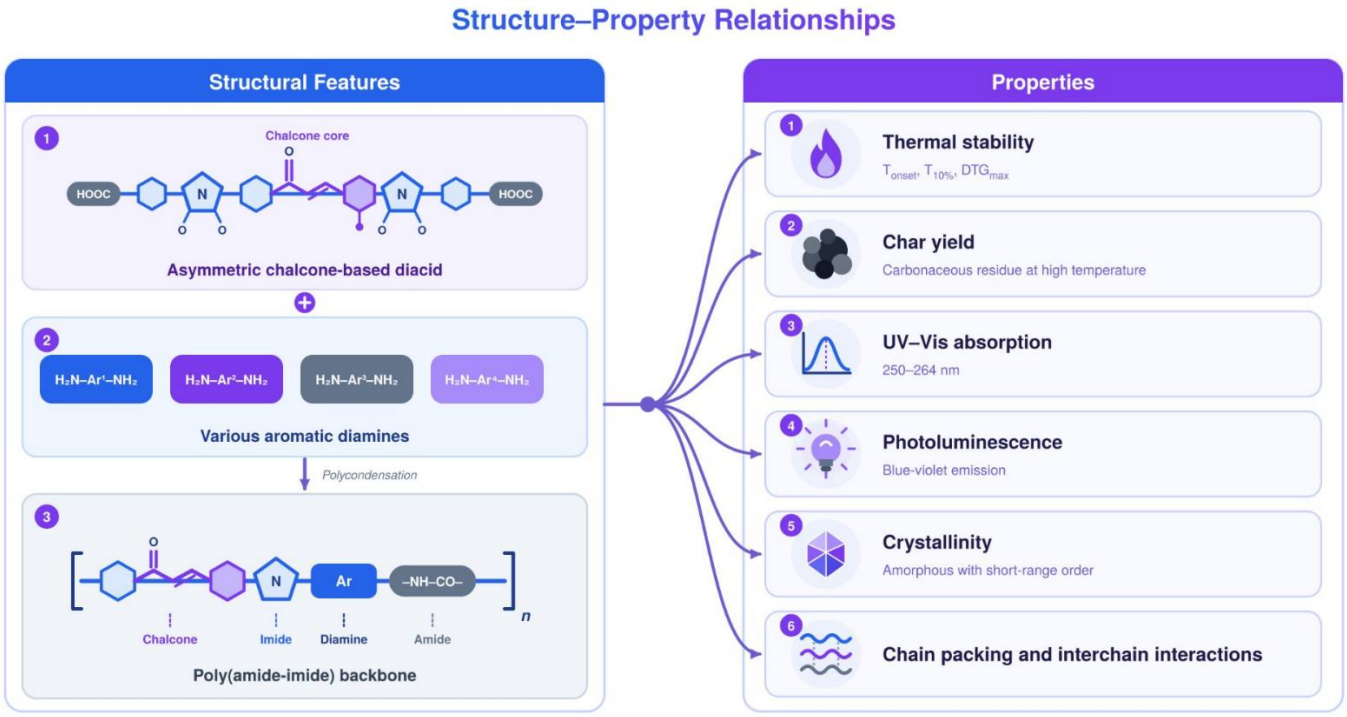


Figure 4. Schematic structure–property relationship map for the synthesized PAIs, illustrating how the asymmetric chalcone-based diacid and different aromatic diamines influence thermal stability, char yield, UV absorption, photoluminescence, crystallinity, and chain packing.

The proposed thermal degradation mechanism, illustrated in Figure 5, involves the sequential cleavage of amide linkages, imide ring opening, and breakdown of the chalcone units, ultimately yielding volatile products and a stable carbonaceous residue.

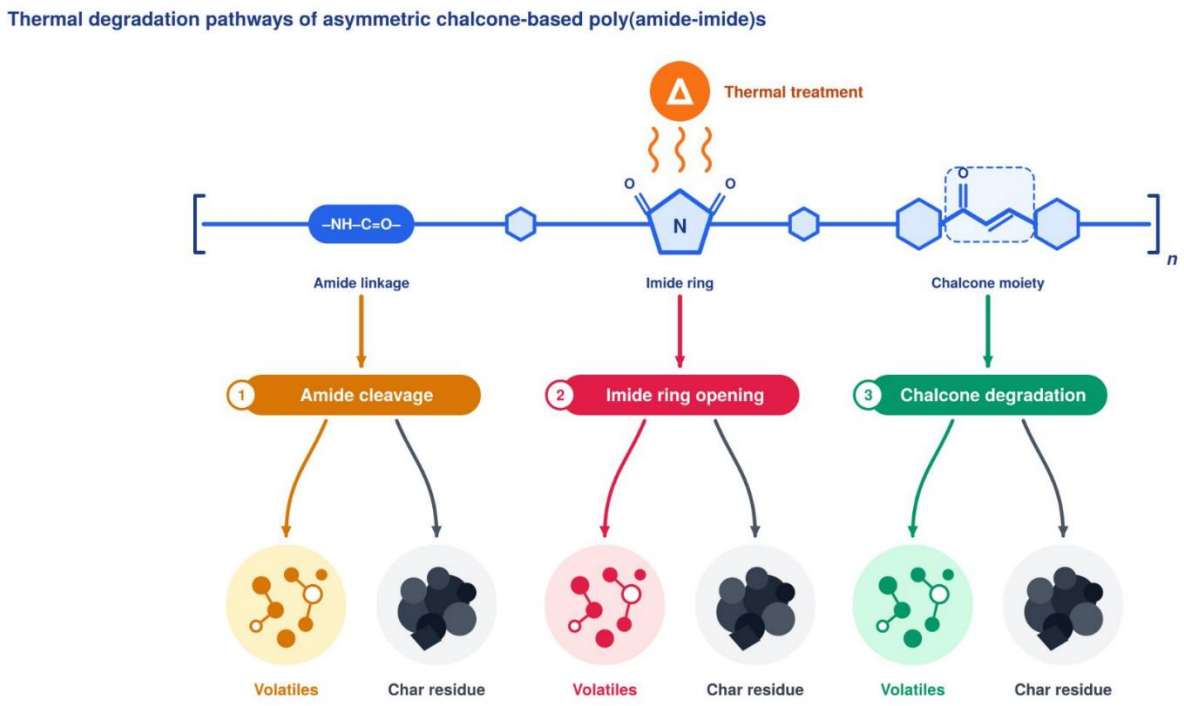


Figure 5. Proposed thermal degradation mechanism of the asymmetric chalcone-based poly(amide-imide)s. The degradation proceeds through cleavage of amide bonds, opening of imide rings, and breakdown of the chalcone moiety, leading to the release of volatile fragments and the formation of a stable aromatic carbonaceous residue (char).

3.4. Optical Properties

The UV–Vis absorption spectra of the PAIs were recorded in DMSO solution (Figure 6). All four polymers exhibited primary absorption in the ultraviolet region, with λ_max values summarized in Table 5.

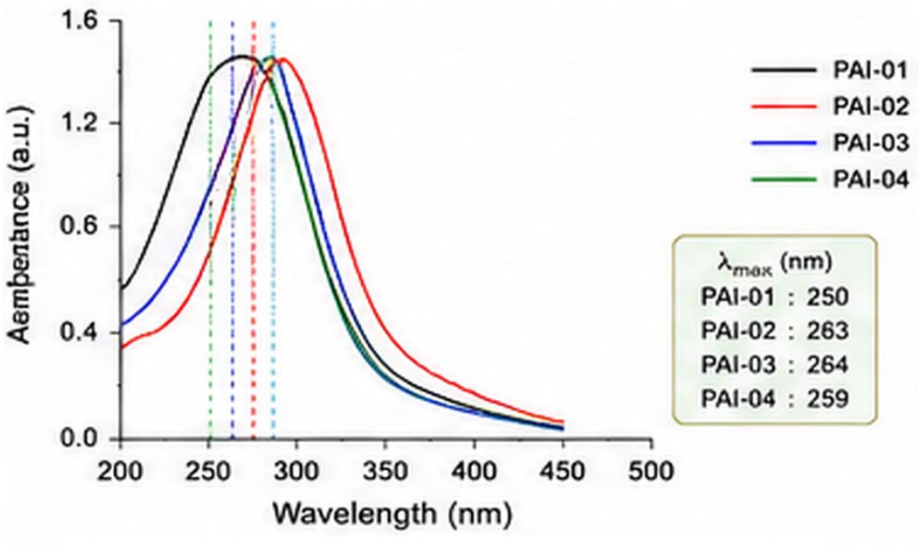


Figure 6. UV–Vis absorption spectra of the synthesized poly(amide-imide)s PAI-01 to PAI-04 in DMSO. The absorption maxima are observed in the range 250–264 nm.

Table 5. UV–Vis absorption maxima of PAI-01 to PAI-04.

PAIs	λ_{max}
PAI-01	250 nm
PAI-02	263 nm
PAI-03	264 nm
PAI-04	259 nm

The absorption in this region arises from π→π* transitions within the aromatic structures. The amide and imide carbonyl groups influence the transition energy by modifying electron flow and creating distinct electronic environments. The absorption wavelengths of PAI-02 and PAI-03 are red-shifted compared to PAI-01, indicating changes in delocalization and the electronic surroundings of the aromatic and carbonyl units.

Photoluminescence (PL) spectra were recorded under excitation at 365 nm (Figure 7). The emission maxima are listed in Table 6.

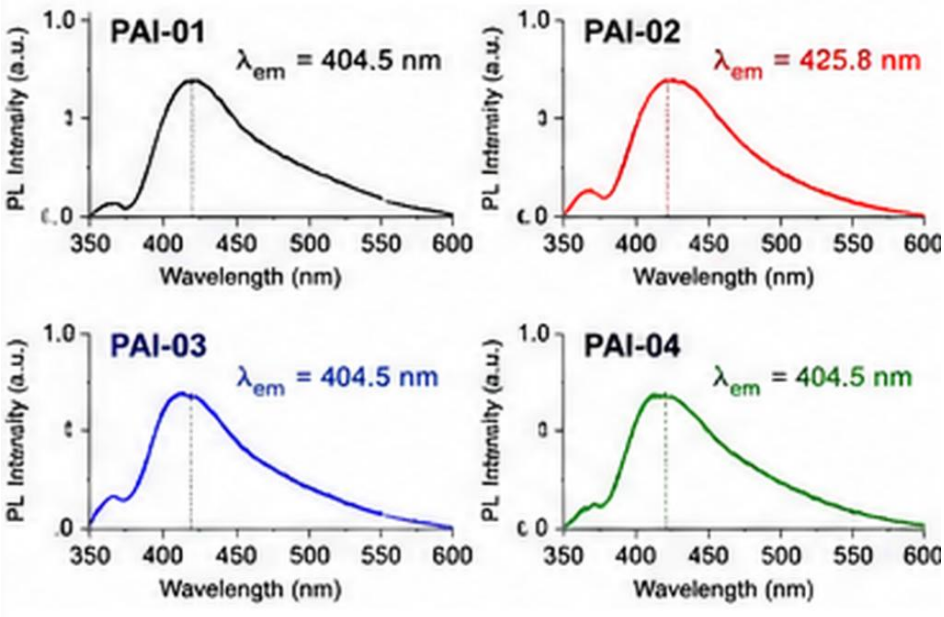


Figure 7. PL emission spectra of the synthesized poly(amide-imide)s PAI-01 to PAI-04 under excitation at 365 nm. PAI-01, PAI-03, and PAI-04 show emission maxima at 404.5 nm, while PAI-02 exhibits a red-shifted emission at 425.8 nm.

Table 6. PL emission maxima of PAI-01 to PAI-04.

$$E = \frac{hc}{\lambda}$$

PAIS	λ-em(nm)
PAI-01	404.5 nm
PAI-02	425.8 nm
PAI-03	404.5 nm
PAI-04	404.5 nm

PAI-01, PAI-03, and PAI-04 exhibited identical emission maxima at 404.5 nm, indicating that their chromophore excited-state energy levels are similar despite differences in molecular structure. PAI-02 showed a red-shifted emission at 425.8 nm, corresponding to a lower photon energy. This red-shift indicates that the energy gap between the excited state and ground state is smaller in PAI-02, which can be attributed to enhanced electron delocalization, modified donor–

acceptor arrangements, altered chromophore polarity, chain organization, and differences in excited-state stability. The comparison of UV–Vis and PL peak positions is shown in Figure 8.

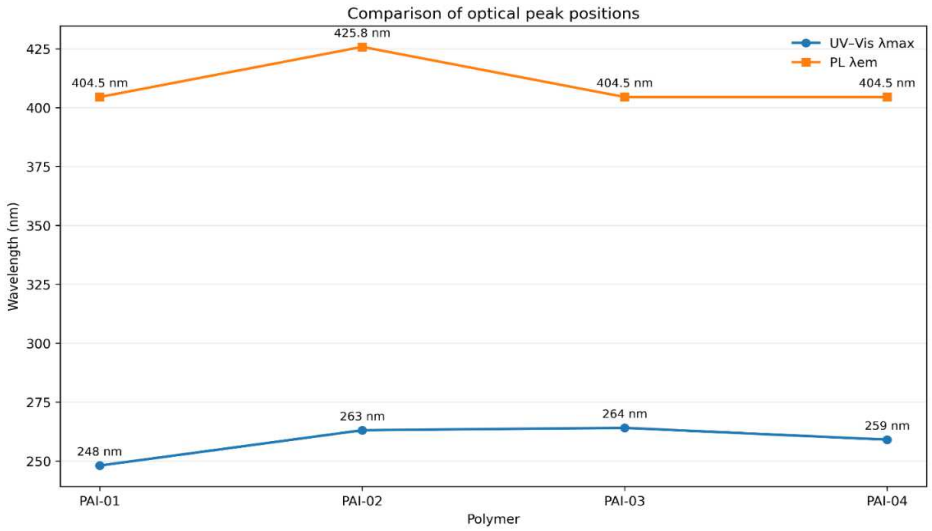


Figure 8. Comparison of the optical peak positions of PAI-01 to PAI-04: UV–Vis λ_max values (250–264 nm) and PL λ_em values (404.5–425.8 nm).

3.5. X-ray Diffraction (XRD) Analysis

The XRD patterns of the PAIs (Figure 9) show broad halos with a few weak diffraction peaks, indicating that the polymers are predominantly amorphous with localized short-range order. The presence of multiple aromatic segments, strong interchain interactions through amide and imide groups, and inflexible chain structures prevent the formation of extensive long-range crystallinity.

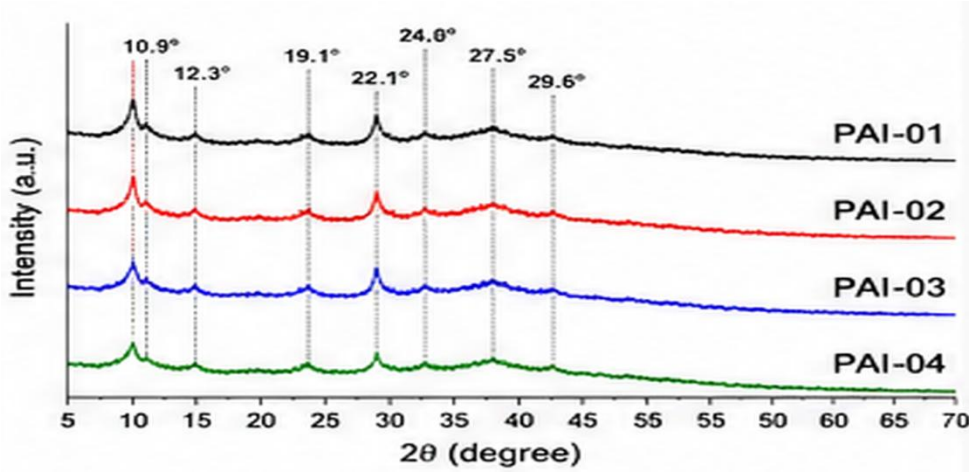


Figure 9. XRD patterns of the synthesized poly(amide-imide)s PAI-01 to PAI-04, showing predominantly amorphous structures with localized short-range order.

The asymmetric nature of the diacid monomer further disrupts chain packing, leading to disordered regions and small ordered domains. The XRD results confirm that the solid-state structure of these polymers consists of a combination of disordered (amorphous) regions and localized short-range order.

3.6. Overall Structure–Property Relationships

The properties of the four PAIs are compared in Table 7. The results demonstrate that the asymmetric chalcone-based diacid, in combination with different diamine structures, significantly influences thermal stability, char formation, UV absorption, photoluminescence, and crystallinity**.**

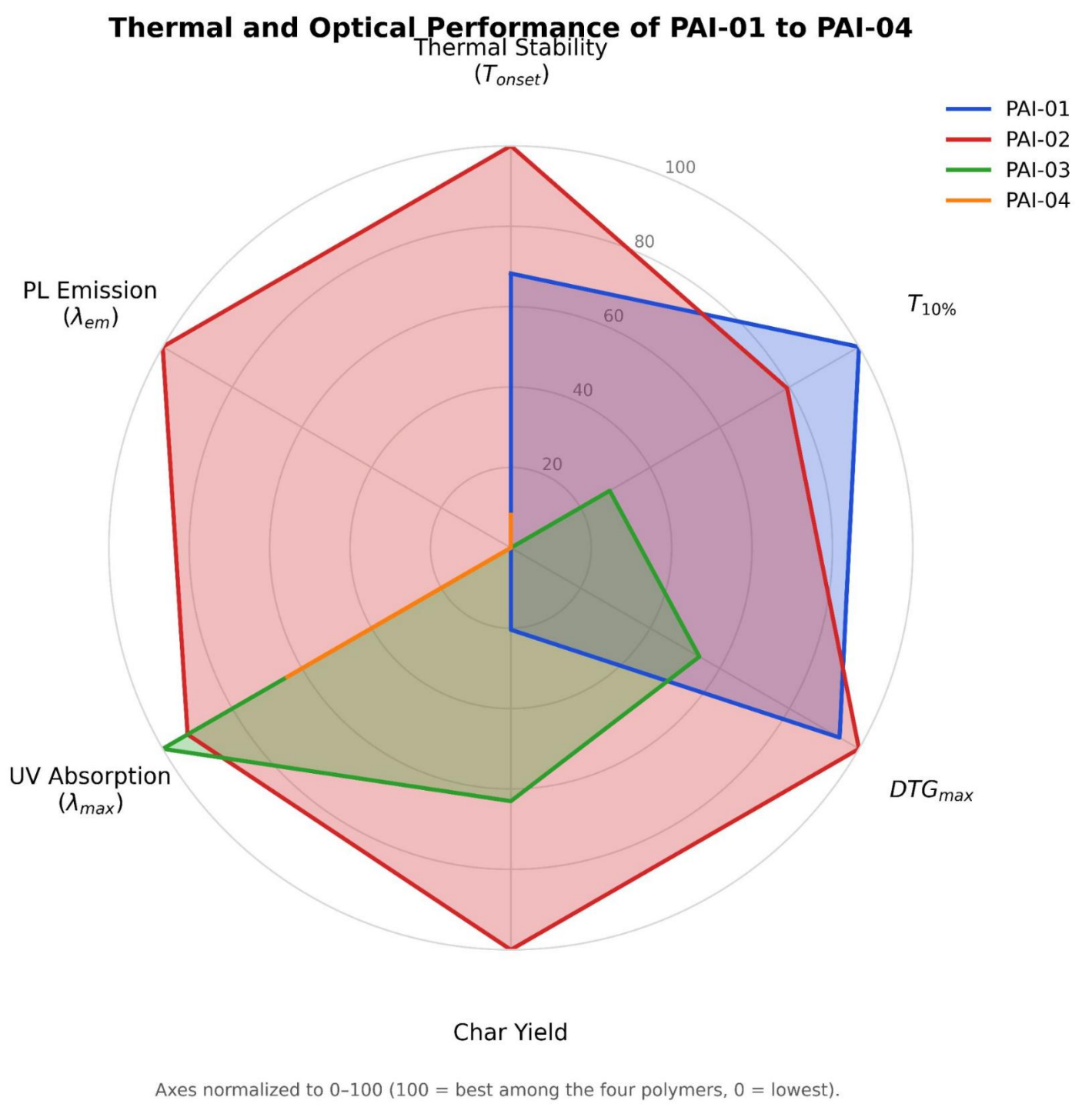
A comprehensive comparison of the thermal and optical properties of the four polymers is presented in Figure 10 as a radar chart, highlighting the balanced performance of PAI-02 and the distinct optical behavior of PAI-02 compared to the other samples.

Table 7. Comparison of key properties of PAI-01 to PAI-04.

Properties	**PAI-01**	**PAI-02**	**PAI-03**	**PAI-04**
UV absorption	250 nm	263 nm	264 nm	259 nm
Main emission	404.5 nm	425.8 nm	404.5 nm	404.5 nm
T_{onset}	Very high	Highest	Lower down	Average
$T_{5\%}$	Very high	Highest	Lower down	Average
$T_{10\%}$	Highest	Very high	Average	Lowest
DTG_{max}	Very high	Highest	Average	Lowest
residue	Average	Highest	high	Lowest
Overall result of the thermal analysis	Very well	The Best	Medium with high char	Lower than other examples
Key optical	Blue emission	Blue emission	Blue emission	Blue emission

Properties	PAI-01	PAI-02	PAI-03	PAI-04
characteristic		to red-shift		

352



353

Figure 10. Radar chart comparing the overall thermal and optical performance of PAI-01 to PAI-04. Axes represent T_onset, T_{10}%, DTG_max, char yield, UV λ_max, and PL λ_em, normalized to a 0–100 scale with the best performance at the outer edge. The data are based on the values reported in Tables 4, 5, and 6.

PAI-02 was identified as the most promising candidate for applications requiring a combination of high thermal stability and blue-violet photoluminescence. Its high char yield, high DTG_max, and red-shifted emission make it particularly attractive for advanced materials. The study clearly demonstrates that molecular structure, including symmetry, chain organization, and chain interactions, governs the simultaneous thermal and photophysical properties of this polymer family.

A comparison of the thermal and optical properties of the synthesized PAIs with analogous chalcone-based poly(amide-imide)s reported in the literature is presented in Table 8, highlighting the unique combination of high char yield and tunable blue-violet emission achieved in this work.

Table 8. Comparison of thermal and optical properties of the synthesized PAIs (PAI-01–PAI-04) with analogous chalcone-based and related poly(amide-imide)s reported in the literature.

Polymer / Reference	Diacid / Monomer Type	Diamine Type	T_onset (°C)	T_{10}% (°C)	Char Yield (%)	λ_em (nm)
PAI-02 (This work)	Asymmetric chalcone-based diimide-diacid	Diamine 4b	462	491	59.8 (at 800 °C)	425.8
PAI-01 (This work)	Asymmetric chalcone-based diimide-diacid	Diamine 4a	442	508	43 (at 800 °C)	404.5
PAI-03 (This work)	Asymmetric chalcone-based diimide-diacid	Diamine 4c	399	449	52 (at 800 °C)	404.5
PAI-04 (This work)	Asymmetric chalcone-based diimide-diacid	Diamine 4d	404.2	425.6	38.7 (at 800 °C)	404.5
Faghihi & Mozafari [32]	Symmetric chalcone-based diacid (1,3-bis[4,4′-bis(trimellityimido)phenyl]-2-propenone)	Various aromatic diamines	-	-	-	-

Faghihi & Moghanian [33]	Symmetric 4,4′-diaminochalcone + N-trimellitylimido-L-amino acids	-	-	-	-	-
Grabiec et al. [34]	Oxadiazole/pyridine-based dianhydrides	2,5-bis(4-aminophenyl)-1,3,4-oxadiazole	510-437	-	-	453-417

4. Future Perspectives

The present study establishes a clear structure–property relationship for a novel family of asymmetric chalcone-based poly(amide-imide)s, but it also opens several promising avenues for future research. The combination of high thermal stability and tunable photoluminescence observed in these polymers suggests their potential for advanced applications, such as optoelectronic devices, sensors, and high-performance coatings. However, further investigations are necessary to fully exploit their capabilities.

First, expanding the library of asymmetric diimide-diacids by varying the position and nature of substituents on the chalcone core could provide deeper insights into how electronic effects and steric hindrance influence both thermal degradation pathways and emission characteristics. For instance, introducing electron-donating or electron-withdrawing groups at different positions on the aromatic rings may allow fine-tuning of the HOMO–LUMO gap and thus the emission color.

Second, the diamine component offers a vast design space. In this work, four different diamines were used, but many other aromatic diamines with varying flexibility, symmetry, and heteroatom content could be explored. This would help establish more general rules for optimizing char yield and thermal stability while maintaining desirable optical properties. Additionally, incorporating diamines with specific functional groups (e.g., sulfone, ether, or fluorene moieties) could lead to polymers with enhanced solubility, processability, or even stimuli-responsive behavior.

Third, computational studies such as density functional theory (DFT) calculations could complement experimental findings by providing molecular-level understanding of the electronic

transitions, excited-state dynamics, and degradation mechanisms. Such theoretical insights would be invaluable for the rational design of next-generation PAIs with targeted properties.

Fourth, the photoluminescence properties of these polymers warrant further investigation. Measuring quantum yields, studying solvent effects, and examining aggregation-induced emission (AIE) behavior could reveal new functionalities. The red-shifted emission of PAI-02, in particular, suggests that structural asymmetry can be used as a tool to modulate emission color, potentially enabling the development of blue-to-green emitting materials.

Fifth, the thermal degradation behavior should be studied in more detail using techniques such as TGA-FTIR or TGA-MS to identify the volatile products and elucidate the degradation mechanism. This would not only enhance our understanding of the structure–stability relationship but also guide the design of polymers with even higher char yields and thermal resistance.

Finally, practical applications of these PAIs should be explored. For example, they could be tested as components in organic light-emitting diodes (OLEDs), as dielectric materials, or as membranes for gas separation. Their good solubility in polar aprotic solvents makes them suitable for solution processing, which is advantageous for thin-film fabrication. Additionally, the presence of chalcone moieties offers opportunities for photo-crosslinking, which could be exploited to create stable crosslinked films with enhanced mechanical and thermal properties.

The promising combination of thermal stability and tunable photoluminescence in these PAIs opens several avenues for future research, as summarized in Figure 11. These include the development of OLEDs and light-emitting devices, chemical and optical sensors, gas separation membranes, photo-crosslinked high-performance coatings, DFT-based excited-state calculations, and detailed thermal degradation analysis using TGA-FTIR or TGA-MS.

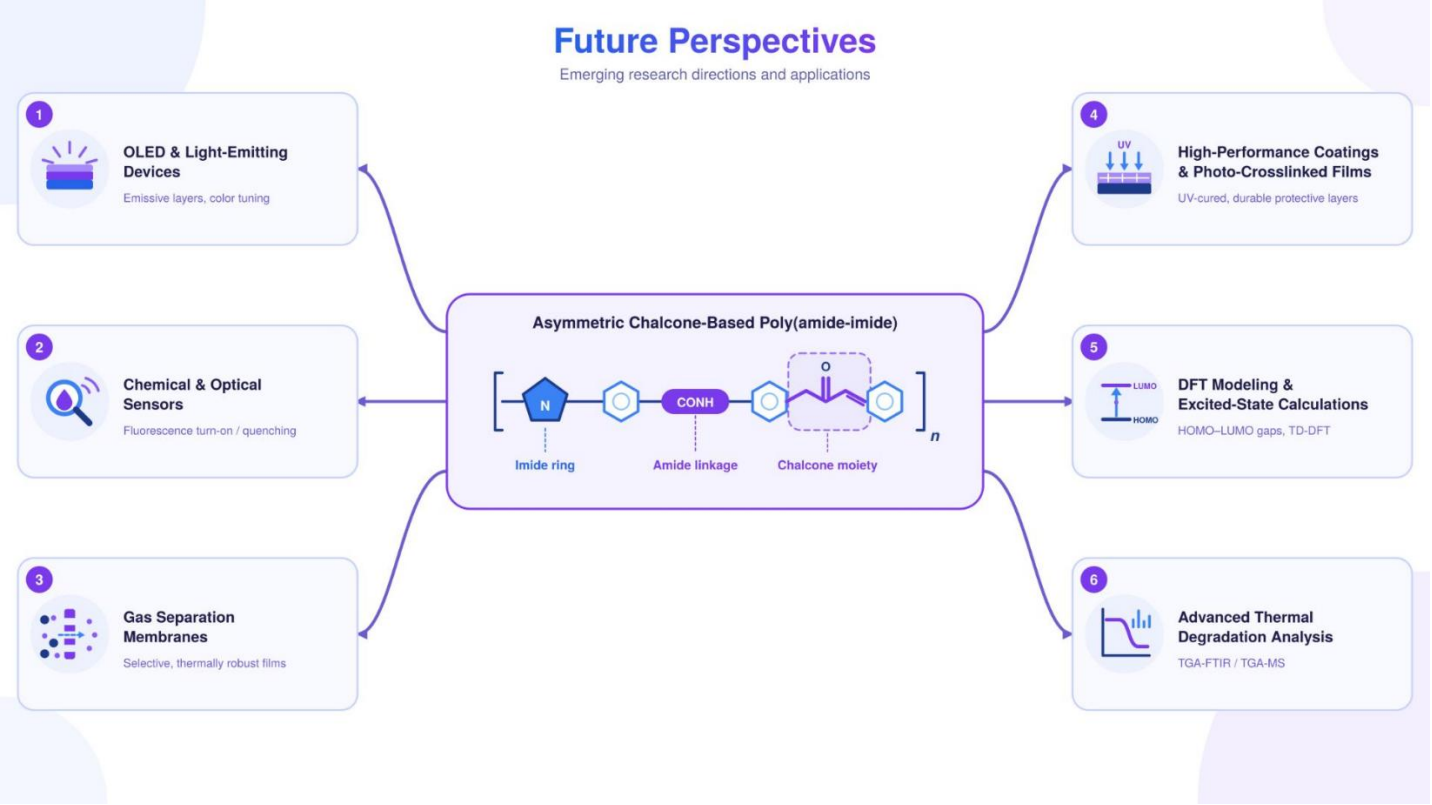


Figure 11. Schematic overview of future research directions and potential applications of asymmetric chalcone-based poly(amide-imide)s. The central polymer backbone branches into six areas: optoelectronic devices (OLEDs), chemical and optical sensors, gas separation membranes, high-performance and photo-crosslinked coatings, DFT computational modeling, and advanced thermal degradation analysis (TGA-FTIR/MS).

In summary, the asymmetric chalcone-based poly(amide-imide)s reported here represent a versatile platform for the development of high-performance materials. Future work should focus on broadening the monomer scope, deepening the mechanistic understanding, and exploring real-world applications to fully realize the potential of this class of polymers.

5. Conclusions

In this study, a novel asymmetric diimide-diacid, 3,4′-bis(3-N-trimellitimido)chalcone (6), was successfully synthesized and employed as a key building block for the preparation of a series of aromatic poly(amide-imide)s (PAI-01–PAI-04) via solution polycondensation with four structurally different aromatic diamines. The synthetic route was straightforward and efficient, and the resulting polymers were fully characterized by FT-IR, ^{1}H NMR, UV–Vis, PL, XRD, TGA, and DTG. The introduction of asymmetry into the diacid monomer, combined with

variation of the diamine architecture, provided a powerful means to modulate chain packing, thermal degradation pathways, and photophysical behavior.

Thermal analysis revealed that all four polymers possess excellent thermal stability, with onset degradation temperatures above 400 °C. Among them, PAI-02 exhibited the highest thermal resistance, characterized by the highest T_onset (462 °C), the highest DTG_max (528.3 °C), and the highest char yield at 800 °C (59.8%). In contrast, PAI-01 showed the highest T_{10}% value (508 °C), indicating superior stability during the later stages of degradation. These results demonstrate that the onset of degradation and the ability to form a stable carbonaceous residue are governed by different structural factors, and that structural asymmetry plays a crucial role in directing degradation pathways.

Optical investigations showed that all polymers absorb in the ultraviolet region (250–264 nm) and emit primarily in the violet–blue region. PAI-01, PAI-03, and PAI-04 exhibited identical emission maxima at 404.5 nm, whereas PAI-02 displayed a red-shifted emission at 425.8 nm, attributed to enhanced electron delocalization and altered excited-state dynamics. XRD analysis confirmed that the polymers are predominantly amorphous with localized short-range order, consistent with the presence of asymmetric units that disrupt long-range chain packing.

Overall, this work establishes a clear structure–property relationship for asymmetric chalcone-based poly(amide-imide)s. The asymmetric diacid, in combination with the diamine structure, controls thermal stability, char formation, UV absorption, and photoluminescence. Among the synthesized polymers, PAI-02 emerges as the most promising candidate for applications requiring a combination of high thermal stability and blue-violet photoluminescence. These findings not only expand the family of high-performance PAIs but also provide valuable design guidelines for the development of advanced polymeric materials with tailored thermal and optical properties.

Declarations

Author contribution statements

Matin Varcheh ,

Khalil Faghihi[a]

Clinical Trial Number

not applicable

Ethics approval and consent to participate

Not applicable

Consent for publication

Not applicable

Availability of data and material

Data available within the article or its supplementary materials

The authors confirm that the data supporting the findings of this study are available within the article [and/or its supplementary materials].

Competing interests

The authors declare that they have no competing interests

Funding

Any funding source had no role in the design of this study and will not have any role during its execution, analyses, interpretation of the data, or decision to submit results

Disclosure statement

No potential conflict of interest was reported by the authors.

Acknowledgments

Organic Polymer Chemistry Research Laboratory, Department of Chemistry, Faculty of Science, Arak University, 38158-879, Arak, Iran.

Reference

1. Li, L., et al., *From molecular design to practical applications: strategies for enhancing the optical and thermal performance of polyimide films.* Polymers, 2024. **16**(16): p. 2315.
2. Zhu, G., et al., *Synthesis and characterization of poly (amide-imide) s with high Tg and low CTE derived from isomeric amide-containing diamines.* European Polymer Journal, 2022. **179**: p. 111558.
3. Wang, L., et al., *Tailoring Molecular Structures of Polyimides for Frontier Applications.* Advanced Materials, 2026: p. e73720.
4. Nagella, S.R. and C.-S. Ha, *Structural designs of transparent polyimide films with low dielectric properties and low water absorption: a review.* Nanomaterials, 2023. **13**(14): p. 2090.
5. Yang, L., et al., *Molecular structure engineering of polyaramid dielectric films for enhanced high-temperature energy storage performance.* Reactive and Functional Polymers, 2026: p. 106944.
6. Yaling, G., W. Jing, and G. Qianqian, *Lignin-inspired aromatic–aliphatic copolyesters with tunable thermomechanical properties for potential teaching material aid.* Journal of Macromolecular Science, Part A, 2026: p. 1-11.
7. Shen, H., et al., *Modulating Crystallization Behavior to Improve Melt Processability and Mechanical Performance in PCT Copolyesters via Benzenedimethanol Incorporation.* ACS Applied Polymer Materials, 2026. **8**(17): p. 15528-15539.

8. Zhou, W., et al., *Gating hole back-transfer with molecular spacers programs rapid micropollutant decontamination.* Nature Communications, 2026.
9. Smith, L.O.I., *Towards High Throughput Simulations and Machine Learning to Predict Polymer Phase Behaviour*. 2025, The University of Manchester (United Kingdom).
10. Muniz, C., *Two-Coordinate Coinage Metal Complexes for Solar Fuels and Organic LED Chemistry*. 2023, University of Southern California.
11. Sharma, G., et al., *Study of Excited-State Dynamics in Methylene Blue and Methyl Orange: Ultrafast Spectroscopic Insights.* ChemistrySelect, 2026. **11**(37): p. e74724.
12. Zhang, R., et al., *Advances in Luminescent Polyurethanes: Materials Design and Emission Modulation.* Advanced Optical Materials, 2026: p. e71707.
13. Caballero, E., et al., *Expanding the Subporphyrazine Chromophore by Conjugation of Phenylene and Vinylene Substituents: Rainbow SubPzs.* The Journal of Organic Chemistry, 2020. **85**(4): p. 1948-1960.
14. Mathius, M.A., et al., *Linear Extension of Carbaporphyrin Chromophores: Synthesis, Protonation, and Metalation of Anthro [2, 3 ‐b] carbaporphyrins: Evidence for 30π-Electron Aromatic Circuits in a Palladium (II) Complex.* The Journal of organic chemistry, 2024. **89**(1): p. 124-140.
15. Paul, D., et al., *Revealing the Role of Electronic Effect to Modulate the Photophysics and Z ‐Scan Responses of o ‐Locked GFP Chromophores.* The Journal of Physical Chemistry B, 2025. **129**(2): p. 692-711.
16. Barkale, H.V., et al., *Multiparametric Analysis of Heavy Metal Pollutants: From Paper-Based Devices to Photodetector Platforms for On-Field Sensing Applications.* Journal of Materials Chemistry C, 2026.
17. Dwivedi, R. and R.K. Dwivedi, *A comprehensive review on conducting polymers for multifaceted applications.* Journal of Inorganic and Organometallic Polymers and Materials, 2026. **36**(7): p. 3521-3559.
18. Kurşun Aktar, B.S., et al., *Design, in Vitro Biological Activities and Molecular Dynamics Simulations of Novel Chalcone and Pyrazole Derivatives Targeting α-Glucosidase and PPAR-γ as Antidiabetic Agents.* ACS omega, 2026. **11**(33): p. 49464-49479.
19. Ozanique, P.R., et al., *Bioactive Natural and Synthetic Chalcones: Brazil as a Research Powerhouse in Discovery and Innovation.* ChemMedChem, 2026. **21**(15): p. e70367.
20. Bebek, G.C., *Evaluation of the possible anti-cancer effect of novel synthesized fluoro-and methoxy-substituted chalcone compounds in different cell lines*. 2023, Erzincan Binali Yıldırım University.
21. Rashmi, et al., *Chalcone-Incorporated Methyl Cellulose Based Polymer Composite Films With Tunable Optical and Electrical Properties.* SPE Polymers, 2026. **7**(4): p. e70066.
22. AHLATCIOĞLU, E., *Synthesis of conducting polymers and investigation of their electrical properties.* 2015.
23. Tian, J.-S., et al., *Catalytic enantioselective construction of spiro stereocenters: recent advances and perspectives.* Science China Chemistry, 2026: p. 1-20.
24. Lenihan, J., *Synthesis of Diverse Cyclobutane Scaffolds and Utilization in Total Synthesis and Medicinal Chemistry*. 2024, Boston University.
25. Mahdy, A., et al., *Soft and rigid imide-based benzoxazines as precursors to high-performance polybenzoxazines: synthesis, thermal behavior, and tunable photoluminescent properties.* Chinese Journal of Polymer Science, 2026: p. 1-23.
26. Zhan, J., et al., *From Molecular Design to Applications: A Comprehensive Review on Modifying Bismaleimide-Triazine Resin Substrates for Advanced Electronic Packaging and Communications.* ACS Applied Electronic Materials, 2026.

27. Ma, W., et al., *The influence of different amounts of fluorine-containing groups in PI replacing corresponding methyl groups on thermal and optical properties.* Journal of Materials Chemistry C, 2026.
28. Bapat, S.P., *Processable high performance polymers: synthesis, characterization and application.* 2007.
29. Kim, B.-T., J.-C. Chun, and K.-J. Hwang, *Synthesis of dihydroxylated chalcone derivatives with diverse substitution patterns and their radical scavenging ability toward DPPH free radicals.* Bulletin of the Korean Chemical Society, 2008. **29**(6): p. 1125-1130.
30. Goyal, K., et al., *Chalcones: A review on synthesis and pharmacological activities.* Journal of Applied pharmaceutical science, 2021. **11**(S1): p. 001-014.
31. Suwito, H., et al., *Chalcones: synthesis, structure diversity and pharmacological aspects.* J. Chem. Pharm. Res, 2014. **6**(5): p. 1076-1088.
32. MOZAFARI, K.F.a.Z., *Synthesis and Properties of Novel PhotosensitivePoly(amide-imide)s Containing Chalcone Moiety and Aromatic Diamines in the Main Chain.* Turk J Chem, 2008. **32**: p. 673-683.
33. Moghanian, K.F.H., *Synthesis and characterization of optically active poly(amide-imide)s containing photosensitive chalcone units in the main chain.* Chinese Journal of Polymer Science, 2010. **28**: p. 695-704.
34. Eugenia Grabiec , M.K., Ewa Schab-Balcerzak, *Poly(amide imides) and poly(ether imides) containing 1,3,4-oxadiazole or pyridine rings: characterizations and optical properties.* The Journal of Physical Chemistry A | ACS Publications, 2009: p. 26;113(8):1481-8.